Journal of Nepal Mathematical Society (JNMS)
ISSN: 2616-0153 (Print), 2616-0161 (Online)
Vol. 7, Issue 2, 2024 (Dec.): 08-21
DOI: https://doi.org/10.3126/jnms.v7i2.73100

Research Article
Received Date: July 18, 2024
Accepted Date: Dec. 11, 2024
Published Date: Dec. 29, 2024

Impact of Effective Viscosity on Blood Flow through Sinusoidal Stenosed Curved Artery

Chudamani Pokharel[1,2], Jeevan Kafle[1], Chet Raj Bhatta[1,*]

[1]Central Department of Mathematics, Tribhuvan University, Kathmandu, Nepal
[2]Dhawalagiri Multiple Campus, Tribhuvan University, Baglung, Nepal
[*]Correspondence to: Chet Raj Bhatta
Email: chet.bhatta@cdmath.tu.edu.np

Abstract: *Atherosclerosis induced narrowing of arteries reduces blood flow to critical regions, contributing to conditions such as ischemia, angina, and strokes. Curvature is observed in blood vessels at various locations. The sinusoidal stenotic surface provides additional curvature and a point of maximum shear, which varies with the cross-section. This research extends the cylindrical form of the Navier-Stokes equations in a polar coordinate system to incorporate effective viscosity and axial curvature, enabling the analysis of blood flow behavior in curved arteries with sinusoidal stenosis. The blood flow behavior was studied by taking different blood parameters using an extended blood flow model. Moreover, aspects of blood flow such as velocity profile, volumetric flow rate, pressure drop, and shear stress have been studied in relation to blood flow around curved arteries with sinusoidal stenosis, variations in the radii of the artery, thickness of the stenosis, hematocrit, and viscosity. The findings reveal that increasing the values of curvature, hematocrit, viscosity, and thickness of stenosis can quickly reduce velocity and volumetric flow rate while amplifying shear stress and pressure drop. This research considers flow conditions consistent with prior studies and opens routes for exploring unsteady and three-dimensional effects in similar geometries.*

Keywords: Arterial stenosis, Blood viscosity, Curvature, Velocity profile, Volumetric flow rate, Pressure drop, Shear stress

1 Introduction

The deposition of cholesterol, fatty particles, and other foreign substances forms atherosclerotic plaque, while abnormal tissue development causes stenosis, unusual hemodynamic conditions lead to aberrant biological reactions, closely linking blood vessel flow to cardiovascular disorders [10, 18, 23, 26, 34]. Stenosis in an artery typically results from the buildup of cholesterol-laden plaque within its walls, causing a narrowing of the blood passage and a loss of elasticity, which can lead to stroke and heart attack [7, 12, 30, 33]. The primary factors influencing blood flow in the stenosed section of the artery include erythrocyte deformability, wall shear stress, hematocrit levels, and blood viscosity [16]. Understanding fluid dynamical features such as velocity profile, velocity gradient, shear stress, blood pressure drop, red cell deformability, and boundary conditions is crucial for the diagnosis and treatment of many diseases [4, 9, 30]. Blood rheology exhibits a dual nature, behaving as a Newtonian fluid under conditions of high shear rates and large artery diameters, but as a non-Newtonian fluid under conditions of low shear rates and small artery radii [15, 17, 21]. The effect of constriction on blood flow parameters, viscosity, and resistance has been studied both theoretically and empirically [7, 11, 20, 42]. The research, involving collaboration between mathematicians and medical researchers, focuses on developing and verifying an equation for projecting hemodynamic factors in stenotic regions, which is crucial for understanding and managing vascular conditions [6, 35, 40, 42].

Curvature in blood vessels introduces bends that alter blood flow dynamics, impacting hemodynamic parameters like velocity, pressure drop, flow rate, and shear stress [29, 30]. Curvature effects in curved coronary arteries influence blood flow and oxygen transport by influencing the types of flow laminar, steady, and phasic resulting in variations in shear stress distribution and pressure gradients along the vessel walls [23, 27]. The effects of hematocrit levels and velocity slip at the arterial wall on pulsatile blood flow in mildly stenotic curved arteries were investigated [3, 27]. Hematocrit concentration, white blood cell count, and platelet count are crucial components of a blood test that assess the density of blood cells relative to the volume of blood, constituting key metrics in an individual's complete blood count (CBC) [24, 25]. The relationship among hematocrit levels, catheter size, and stenosis profoundly affects blood flow dynamics, emphasizing

the critical role of catheterization in medical practice, as demonstrated by studies in catheterized arteries [39]. The impedance of a catheter is influenced by its dimensions, hematocrit levels, and stenosis size, but is mitigated by its geometric characteristics [38]. The study examined the effects of pressure gradients, blood velocity, volumetric flow rate, and wall shear stress on human carotid arteries, finding that reducing hematocrit and viscosity lowers arterial wall shear stress [29]. Higher hematocrit and blood viscosity reduce wall shear stress, leading to a faster heartbeat and vein damage, thereby demonstrating the relationship between hematocrit and the blood pressure gradient [24].

Misra et al. [22] have found analytical formulas for the flow rate, wall shear stress, prissure gradient, velocity distribution, total angular velocity, and resistance to fluid motion. Mandal and Chakravarty [21] demonstrated that blood behaves non-Newtonian in arteries with low shear rates and tiny radii. Harjeet et al. [14] studied as a Newtonian fluid, experience greater shear stress and resistance during narrow catheterization, the resistance increases in direct proportion to the catheter's size and the height of the stenosis. Young and Tasi [42] have created and verified a rough formula to forecast pressure drops in stenotic regions. Santamarina et al. [37] investigated the intricate mechanics of blood flow over curved pathways. The research provided information on cardiovascular physiology and pathology that can be applied to the diagnosis and management of coronary artery disease. Dash et al. [8] examined the relationship between stenosis and curvature to address blood flow issues in a catheterized artery with minimal stenosis and minimal curvature. Padmanabhan and Jayaraman [31] approached a mathematically modeled blood flow issue in a curved stenosed artery by utilizing toroidal coordinate and perturbation theory. Schilt et al. [36] investigated an in vitro flow model consisting of a fluid flowing in a steady condition via a flexible, curved tube. Chakravarty and Chowdhury [5] carried out research on the behavior of blood flow in a curved artery that was stenosed, looking at how the stenosis form affected the flow resistance. Qiu and Trabell [32] investigated the intricate connections between blood flow dynamics, oxygen transport, and vascular biomechanics in curved coronary arteries. Srivastava [40] found that hematocrit, catheter size, and stenosis size all had an effect on the flow parameter via increasing flow resistance. Onitilo and Usman [24] explored the possibility of lowering artery wall shear stress by raising viscosity and hematocrit. Haldar et al. [13] explored the relationship between blood viscosity, hematocrit, wall shear stress, and velocity and blood flow in stenosed arteries. Bali and Awasthi [2] examined the blood's viscosity by measuring its distance from the center and hematocrit. Pokharel et al. [29] studied the blood flow through stenosed curved artery with Einstein viscosity. Verma and Parihar [41] shown that blood viscosity and hematocrit have a linear connection, and that hematocrit may have an impact on blood flow in an artery that had several tiny stenoses. Alizadehard et al. [1] studied blood flow in circular tubes with varying hematocrits, shear rates, and diameters as well as red blood cell deformation in microvessels using a practical-based model.

This research examines blood flow in curved arteries by integrating curvature into the axial Navier-Stokes equations. Velocity, volumetric flow rate, pressure drop, and shear stress are analyzed under Stenotic conditions using an extended model with specific boundary conditions.

2 Model for Blood Flow through Curved Artery

The steady flow of blood through a symmetrically stenosed artery is modeled, assuming damage endothelium layer and incompressible blood. The radii of the artery without and with stenosis are a and b ($b < a$), respectively. The flow is governed by the Navier-Stokes equations in cylindrical coordinates, with dominant axial flow and negligible radial and circumferential components due to symmetry. Effective viscosity is incorporated to capture non-Newtonian blood behavior influenced by hematocrit and plasma viscosity. Analytical results are visualized in graph and used to evaluate velocity, volumetric flow rate, pressure drop, and shear stress, with results validated against established findings.

The governing equations for blood flow in a sinusoidal stenosed artery, incorporating curvature effect along the axial direction in cylindrical polar coordinates (r, θ, z) is [15, 17, 27, 29]

$$\rho\left(\frac{\partial u^z}{\partial t}+u^r\frac{\partial u^z}{\partial r}+\frac{u^\theta}{r}\frac{\partial u^z}{\partial \theta}+u^z\frac{\partial u^z}{\partial z}\right)=-\frac{\partial p}{\partial z}+\mu\left[\frac{1}{r}\frac{\partial}{\partial r}\left(r\frac{\partial u^z}{\partial r}+\frac{\kappa P}{16\mu}\left(b^2-r^2\right)^2\right)+\frac{1}{r^2}\frac{\partial^2 u^z}{\partial \theta^2}+\frac{\partial^2 u^z}{\partial z^2}\right] \tag{1}$$

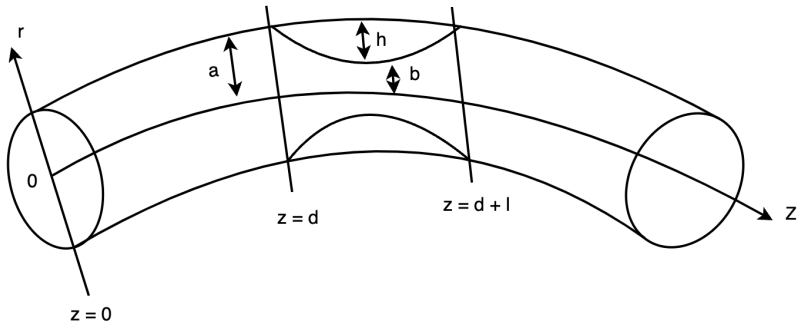

Figure 1: A curved artery with stenosis shown schematically.

Assuming axially symmetric steady flow along the z-axis with $u^\theta = 0$, $u^r = 0$, and $u^z = u(r)$, and considering constant density ρ, the momentum balance equation becomes

$$0 = -\frac{\partial p}{\partial z} + \mu\left(\frac{\partial^2 u}{\partial r^2} + \frac{1}{r}\frac{\partial u}{\partial r} - \frac{\kappa P}{4\mu}(b^2 - r^2)\right) \tag{2}$$

Suppose the pressure term as $P(z) = -\partial p/\partial z$, equation (2) reduces to

$$-P\frac{r}{\mu} = \frac{\partial}{\partial r}\left(r\frac{\partial u}{\partial r} + \frac{\kappa P}{16\mu}\left(b^2 - r^2\right)^2\right). \tag{3}$$

The Einstein coefficient of blood viscosity (the effective viscosity of blood at a radial distance r) is given as [19, 28, 29].

$$\mu(r) = \mu_0\left[1 + \gamma H(r)\right] \tag{4}$$

where μ_0 is the plasma viscosity, γ is a constant that characterizes the dependence of viscosity on hematocrit, $H(r)$ is the hematocrit at radial distance r, so that $\gamma H(r)$ represents the additional viscosity due to the presence of red blood cells which is described by the formula

$$H(r) = \mathcal{H}\left[1 - \left(\frac{r}{a}\right)^n\right] \tag{5}$$

where n is the number of stenosis, we take $n = 1$.

From (4) and (5)

$$\mu(r) = \mu_0\left[1 + \gamma\mathcal{H} - \gamma\mathcal{H}\left(\frac{r}{a}\right)\right]$$

Put $c_2 = \gamma\mathcal{H}$, $c_1 = 1 + c_2$

$$\mu(r) = \mu_0\left[c_1 - c_2\left(\frac{r}{a}\right)\right] \tag{6}$$

2.1 Geometry of stenosis

Figure 1 illustrates the shape of the stenosis formed by the deposition of layer in the interior of an artery with curved cylindrical shape. we have from geometry of stenosis [8].

$$\frac{b}{a} = 1 - \frac{h}{a} L_z \;\; d \leq z \leq d + l \tag{7}$$

where a and b are the radii without and with stenosis, respectively, h is the maximum thickness of the stenosis. The term L_z=$\sin \pi \left(\frac{z-d}{l}\right)$ describes how the radius varies, ensuring smooth transition from 0 at $z = d$ to the maximum height h within $(d, d + l)$ and then decreasing back to 0 at $z = d + l$.

The boundary condition as stated by [8, 17, 26]

$$u = \begin{cases} 0 & at \;\; r = b, \\ 0 & at \;\; r = a, \end{cases}$$

and

$$\frac{\partial u}{\partial r} = 0, \;\; \text{at} \;\; r = 0$$

2.2 Velocity of blood flow in curvature model

Integrating curvature model (3),

$$-P\frac{r^2}{2\mu} + A(z) = r\frac{\partial u}{\partial r} + \frac{\kappa P}{16\mu}\left(b^2 - r^2\right)^2 \tag{8}$$

Using boundary condition, $\frac{\partial u}{\partial r} = 0$ at $r = 0$, the equation (8) yields

$$A(z) = \frac{\kappa P b^4}{16\mu}$$

Then,

$$\frac{\partial u}{\partial r} = -\frac{Pr}{2\mu} + \frac{\kappa P b^2 r}{8\mu} - \frac{\kappa P r^3}{16\mu}$$

On integration

$$u = -\frac{Pr^2}{4\mu} + \frac{\kappa P b^2 r^2}{16\mu} - \frac{\kappa P r^4}{64\mu} + B(z) \tag{9}$$

Using boundary conditions $u = 0$ at $r = b$ in (9) gives

$$B(z) = \frac{Pb^2}{4\mu} - \frac{3Pb^4}{64\mu}$$

After substituting value of $B(z)$

$$u = \frac{P}{4\mu}\left[\left(b^2 - r^2\right) + \frac{\kappa}{16}\left(4b^2r^2 - 3b^4 - r^4\right)\right]$$

$$u = \frac{P}{4\mu_0\left(c_1 - c_2\left(\frac{r}{a}\right)\right)}\left[\left(b^2 - r^2\right) + \frac{\kappa}{16}\left(4b^2r^2 - 3b^4 - r^4\right)\right]$$

Using geometry and binomial expansion, and neglecting the higher power of $\frac{r}{a}$,

$$u = \frac{P\left(1 + \frac{c_2 r}{c_1 a}\right)}{4\mu_0 c_1}\left[\left(a^2\left(1 - \frac{2h}{a}L_z\right) - r^2\right) + \frac{\kappa}{16}\left(4a^2\left(1 - \frac{2h}{a}L_z\right)r^2 - 3a^4\left(1 - \frac{4h}{a}L_z\right) - r^4\right)\right] \tag{10}$$

2.3 Volumetric flow rate in curved artery

The curved artery's volumetric flow rate is

$$Q = \int_0^b 2\pi r dr u = \int_0^b 2\pi r \left[\frac{P}{4\mu} \left(b^2 - r^2\right) + \frac{\kappa P}{64\mu} \left(4b^2 r^2 - 3b^4 - r^4\right) \right] dr$$

After integration and simplification

$$Q = \frac{\pi P b^4}{8\mu} \left(1 - \frac{\kappa b^2}{6}\right) \tag{11}$$

Using the geometry

$$Q = \frac{\pi P a^4 \left(1 - \frac{h}{a} L_z\right)^4}{8\mu} \left(1 - \frac{\kappa a^2}{6} \left(1 - \frac{h}{a} L_z\right)^2\right)$$

Applying the binomial expansion, and neglecting the higher power of h, we have

$$Q = \frac{\pi P a^4 \left(1 + \frac{c_2 r}{c_1 a}\right) \left(1 - \frac{4h}{a} L_z\right)}{8\mu_0 c_1} \left(1 - \frac{\kappa a^2}{6} \left(1 - \frac{2h}{a} L_z\right)\right) \tag{12}$$

2.4 Pressure drop across the stenosis with curvature

Pressure drop across stenosis is

$$\Delta P = \int_d^{d+l} P dz \tag{13}$$

with the help of equation (12) and (13)

$$\Delta P = \int_d^{d+l} \frac{8\mu Q}{\pi a^4 \left[1 - \frac{4h}{a} L_z - \frac{\kappa a^2}{6} + \frac{\kappa a h}{3} L_z + \frac{2\kappa a h}{3} L_z - \frac{4h^2 \kappa}{3} L_z^2\right]} dz$$

Again using the binomial expansion, neglect higher power,

$$\begin{aligned} \Delta P = \int_d^{d+l} \frac{8\mu Q}{\pi a^4} \Bigg(& 1 + \frac{4h}{a} L_z + \frac{\kappa a^2}{6} \\ & - \frac{\kappa a h}{3} L_z - \frac{2\kappa a h}{3} L_z + \frac{4h^2 \kappa}{3} - \frac{4h^2 \kappa}{3} L_z' \Bigg) dz \end{aligned}$$

where

$$L_z' = \cos\left(2\pi \frac{z - d}{l}\right)$$

After integration

$$\Delta P = \frac{4lQ\mu_0 \left(c_1 - c_2(\frac{r}{a})\right)}{\pi a^2} \left(\frac{2}{a^2} + \frac{16h}{\pi a^3} + \frac{\kappa}{3} - \frac{4\kappa h}{\pi a} + \frac{8h^2 \kappa}{3a^2}\right) \tag{14}$$

2.5 Shear stress across the stenosis in curved artery

The stress across the stenosis in the curved artery is

$$\tau = \left[-\mu \frac{\partial u}{\partial r}\right]_{r=b} \tag{15}$$

$$= \left[(-\mu)(-P)\frac{r}{2\mu}\right]_{r=b} = \frac{Pb}{2}$$

Using equations (12) and (15)

$$\tau = \frac{8\mu Q}{\pi a^4 \left[1 - \frac{4h}{a}L_z - \frac{\kappa a^2}{6} + \frac{\kappa a h}{3}L_z + \frac{2\kappa a h}{3}L_z - \frac{4h^2\kappa}{3}L_z^2\right]}\frac{b}{2}$$

$$\tau = \frac{4a\mu_0 Q\left(c_1 - c_2\frac{r}{a}\right)\left(1 - \frac{h}{a}L_z\right)}{\pi a^4 \left[1 - \frac{4h}{a}L_z - \frac{\kappa a^2}{6} + \frac{\kappa a h}{3}L_z + \frac{2\kappa a h}{3}L_z - \frac{4h^2\kappa}{3}L_z^2\right]} \tag{16}$$

3 Results and Discussions

We analyzed blood flow in sinusoidal stenosed arteries allows for a detailed understanding of the hemodynamic changes caused by narrowing. By visualization how factors like velocity, volumetric flow rate, pressure drop, shear stress, and flow patterns are altered in stenotic regions, these models help reveal the complex relationship between artery geometry, fluid dynamics, and disease progression. This results also aids in predicting the severity of blockages, optimizing treatment plans.

3.1 Velocity profile across a curved stenotic artery

Figure 2A displays the velocity distribution has been analyzed for different viscosity levels with radial distance r. The values of the viscosity coefficient μ are $0.4, 0.7, 1.0$, and 1.3 gram mm^{-1} s^{-1}. The radius r varies from 0 to 3 mm. At r =1 mm the velocity u for the viscosity coefficient $0.4, 0.7, 1.0$, and 1.3 gram mm^{-1} s^{-1} are 204.1 mm s^{-1}, 116.9 mm s^{-1}, 81.78 mm s^{-1}, and 62.49 mm s^{-1}, respectively. This indicates that, u is the maximum velocity for a given viscosity coefficient, μ_1=0.4 gram mm^{-1} s^{-1}, at 204.1 mm s^{-1}. Similarly, the minimum velocity is found for the viscosity coefficient, μ_4=1.3 gram mm^{-1} s^{-1}, at 62.49 mm s^{-1}. This observation shows the resistance to flow caused by viscosity, higher viscosity increases the internal friction within the blood, leading to a reduced velocity.

Figure 2B shows the distribution of velocity with radial distance r has been analyzed for various hematocrit values H, specifically $0.1, 0.3, 0.5$, and 0.7, with r ranging from 0 to 3 mm. At r= 1 mm the velocities for hematocrit levels of $0.1, 0.3, 0.5$, and 0.7 are 145.6 mm s^{-1}, 107.5 mm s^{-1}, 86.72 mm s^{-1}, and 72.6 mm s^{-1}, respectively. The velocity distribution is found to be lowest for a hematocrit value of H_4= 0.7, equivalent to 72.6 mm s^{-1}, and highest for hematocrit value of H_1= 0.1, equivalent to 145.6 mm s^{-1}. The behavior reflects the influence of hematocrit on blood flow as hematocrit increases, the increased viscosity leads to greater resistance to flow, slowing the velocity, particularly near the vessel wall, and enhancing the role of viscous dissipation in the flow dynamics.

Figure 2C depicts the distribution of velocity has been examined for different values of curvature κ, which are $0.1, 0.2, 0.3$, and 0.4mm^{-1} s. The radius r of an artery takes values of $0, 1, 2, 3)$ mm. At r = 1 and $\kappa_1 = 0.1$ mm^{-1} s, the velocity is 132.5 mm s^{-1}. As the radius increases, the velocity decreases for the same curvature, approaching zero at r = 2.94 mm and 5.399 mm s^{-1} at r = 3 mm. Similarly, at r = 1 mm and κ = 0.2 mm^{-1} s, the velocity is 108.2 mm s^{-1}, it also becomes approximately zero at r = 2.94 mm and 5.399 mm s^{-1} at r = 3 mm for this curvature. The velocities at r = 0 mm are $127.9, 103.3, 78.63$, and 54 mm s^{-1} for curvature of $0.1, 0.2, 0.3$, and 0.4 mm^{-1} s respectively. This shows that curvature introduces additional resistance to flow as the curvature of the artery increases, the flow is reduced. This effect is more pronounced as the radial distance from the center increases, where the velocity near the walls tends toward zero due to the combined influence of radial distance and curvature. The gradual reduction of velocity with increasing curvature reflects the impact of arterial geometry on blood flow, which influences the pressure and shear stress distributions within the vessel.

Figure 2D, describes the distribution of velocity for different values of viscosity and radius of artery. Viscosity μ takes vlues $(0.4, 0.7, 1.0, 1.3$ gram mm^{-1} s^{-1}. Radius of an artery has values $(0, 1, 2, 3)$ mm. The velocity u at r = 0 and μ_1 = 0.4 gram mm^{-1} s^{-1} is 227.6 mm s^{-1}. As the radius increases the velocity decreases for the same viscosity and becomes 139.8 at r = 2 mm. The velocity at r = 2 mm is 42.45 mm s^{-1} for the viscosity 1.3 gram mm^{-1} s^{-1} and becomes 0 at r = 3 mm for the same viscosity. The velocities

at $r = 1$ mm are $(207.1, 118.5, 81.22, 63.48)$ mm s^{-1} for the viscosity $(0.4, 0.7, 1.0, 1.3)$ gram mm^{-1} s^{-1} respectively. The velocities are 0 at $r = 3$ mm for the viscosities $(0.4, 0.7, 1.0, 1.3)$ gram mm^{-1} s^{-1} respectively. This demonstrates the combined effect of increased internal friction (due to higher viscosity) and the expanding vessel size (increasing radial distance), which together contribute to a significant reduction in velocity, especially near the vessel wall. The flow becomes more constrained as both factors increase, leading to a diminishing velocity profile, which is critical for understanding flow resistance and shear stress in arterial dynamics.

The velocity distribution analysis shows that viscosity, hematocrit, and curvature all significantly influence blood flow. Viscosity has the greatest impact, with higher values leading to the most substantial reduction in velocity due to increased internal friction. Hematocrit follows, as higher red blood cell concentration raises viscosity, thus slowing the flow, especially near the walls. Curvature also plays a role, introducing resistance that constrains flow and reduces velocity, with the effect becoming more pronounced as the radial distance increases.

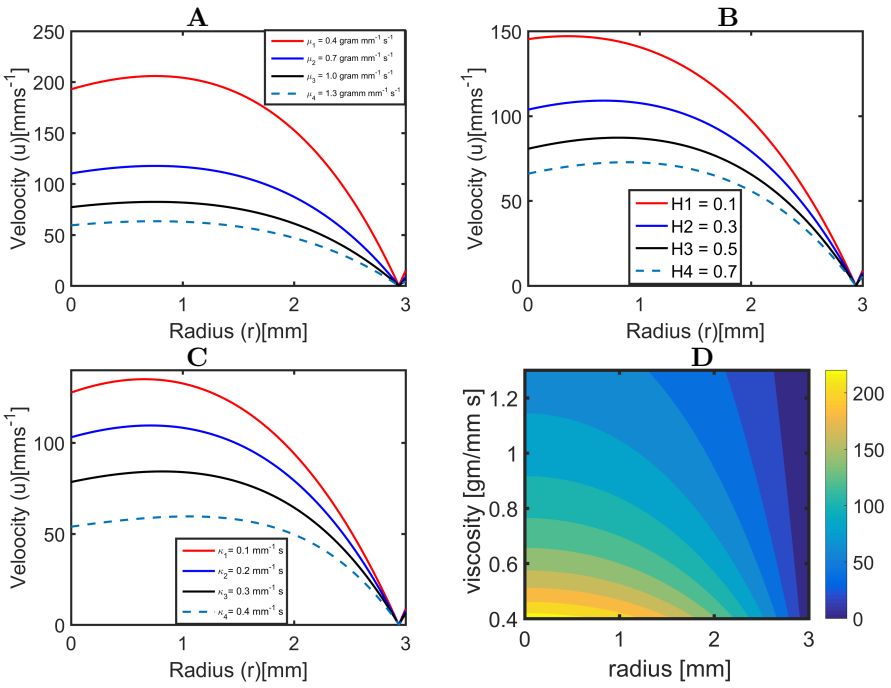

Figure 2: Velocity variations with radial distance for **A:** different viscosities, **B:** various hematocrit, **C:** various curvature, **D:** various viscosity and radius.

3.2 Volumetric flow rate across a curved stenotic artery

Figure 3A shows the volumetric flow rate of blood in an artery (Q) is influenced by both the viscosity of the blood and the height of stenosis within the artery. Viscosity values considered $0.4, 0.7, 1.0$, and 1.3 gram mm^{-1} s^{-1}. The stenosis height ranges from 0 to 0.3 mm. When the stenosis height h is 0, the volumetric flow rates for the respective viscosities are 501 mm^3 s^{-1}, 417.5 mm^3 s^{-1}, 313.1 mm^3 s^{-1}, and 250.5 mm^3 s^{-1}. These values illustrate that an increase in the viscosity of the blood results in a reduction in the volumetric flow rate. The relationship between viscosity and flow rate becomes approximately linear, and higher viscosity results in lower centripetal acceleration and slower fluid flow. When the stenosis height is increased to 0.3 mm, the volumetric flow rates for the respective viscosities are 455.3 mm^3 s^{-1}, 379.5 mm^3 s^{-1}, 284.6 mm^3 s^{-1}, and 227.7 mm^3 s^{-1}. This suggests that the narrowing of the artery becomes the dominant factor affecting flow, diminishing the impact of viscosity. The physical interpretation highlights how stenosis reduces the overall cross-sectional area for blood flow, which restricts the flow more than

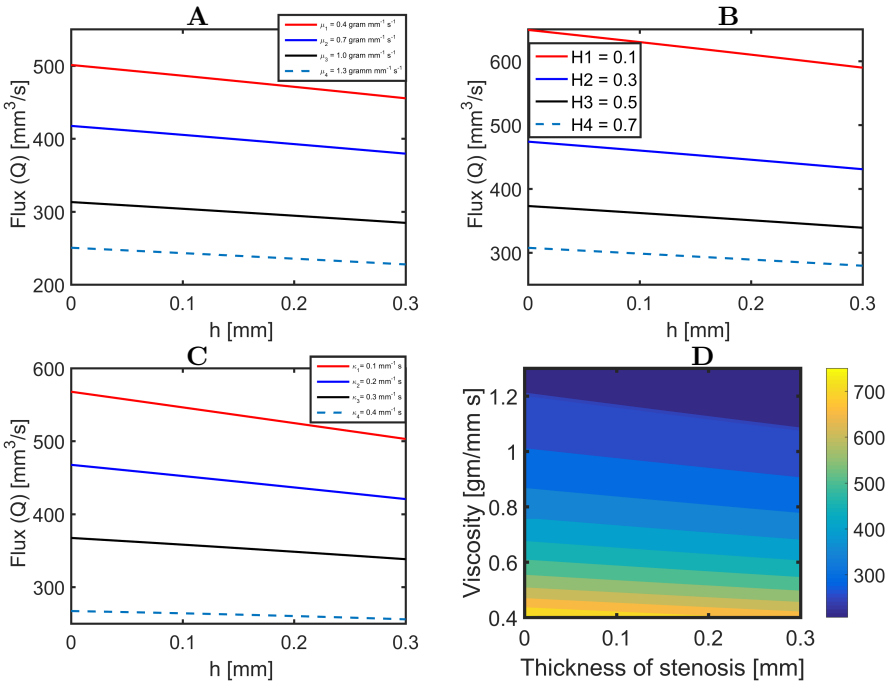

Figure 3: volumetric flow rate variations with thickness of stenosis for **A:** different viscosities, **B:** various hematocrit ,**C:** various curvature, **D:** various viscosity and thickness of stenosis.

viscosity alone. In severely stenosed arteries, the reduction in diameter plays a more significant role in limiting flow than the blood's viscosity.

Figure 3B explains that the volumetric flow rate of blood in an artery (Q) is influenced by both the hematocrit level and the height of stenosis. Hematocrit values of 0.1, 0.3, 0.5, and 0.7 correspond to volumetric flow rates of 648.9 mm^3 s^{-1}, 473.9 mm^3 s^{-1}, 373.1 mm^3 s^{-1}, and 307.6 mm^3 s^{-1}, respectively, when ($h = 0$). This indicates that an increase in hematocrit results in a decrease in volumetric flow rate. When hematocrit levels vary, the resulting curves tend to be linear, with higher hematocrit levels leading to reduced centripetal acceleration and slower fluid flow. At a stenosis height of $h = 0.3$ mm, the volumetric flow rates are 589.8 mm^3 s^{-1}, 430.7 mm^3 s^{-1}, 339.1 mm^3 s^{-1}, and 279.5 mm^3 s^{-1} for hematocrit levels of 0.1, 0.3, 0.5, and 0.7, respectively. This result shows that as the narrowing of the artery increasing the fluid's resistance (due to reduced cross-sectional area), making the effect of hematocrit on the flow rate less significant in the presence of severe stenosis. The overall effect is a higher entropy generation due to increased friction and energy dissipation, which is amplified by both higher hematocrit levels and the presence of stenosis.

Figure 3C the volumetric flow rate(Q) distribution is depicted with respect to the width of stenosis h for various values of curvature. Curvature κ takes the values $0.1, 0.2, 0.3$, and 0.4 mm^{-1} s. The width of stenosis ranges from 0 to 0.3 mm. The volumetric flow rates at h= 0 are 567.8 mm^3 s^{-1}, 467.6 mm^3 s^{-1}, 367.4 mm^3 s^{-1}, and 267.2 mm^3 s^{-1} for the curvature $0.1, 0.2, 0.3, 0.4$ mm^{-1} s, respectively. The volumetric flow rate at h= 0.3 mm are 503 mm^3 s^{-1}, 420.6 mm^3 s^{-1}, 338.3 mm^3 s^{-1}, and 255.9 mm^3 s^{-1} for the curvature $0.1, 0.2, 0.3$, and 0.4 mm^{-1} s, respectively. As the curvature shifts from 0 to 0.4 mm^{-1} s, the flux decrease to $64.8, 47, 29.1$, and 11.3 mm^3 s^{-1} for the height of stenosis $0, 0.1, 0.2$, and 0.3 mm, respectively. This result highlights the importance of both vessel geometry (curvature and stenosis) in regulating blood flow, with more curved and narrowed arteries causing greater flow restriction. The reduction in volumetric flow rate with increasing stenosis height and curvature reflects the physiological impact of arterial remodeling and the complex interplay between vascular geometry, resistance, and shear stress in the human circulatory system.

Figure 3D, describes the combined effect of volumetric flow rate for increased viscosity due to the presence of red blood cells and height of stenosis. The volumetric flow rate at $h = 0$ and $\mu_1 = 0.4$ gram/mm s is 754 mm^3 s^{-1}. As the increased viscosity due to the presence of red blood cells increases, the volumetric flow rate decreases for the constant hematocrit and curvature, then it becomes 384.7 mm^3 s^{-1} at $\mu_4 = 1.3$ gram/mm s and $h = 0.1$ mm. The volumetric flow rate at $\mu_1 = 1.3$ gram/mm s and $h = 0$ is 675.1 mm^3 s^{-1} for the constant hematocrit 0.4 and becomes 384.7 mm^3/s at $h = 0.1$ mm for the same viscosity. The gradual reduction in volumetric flow rate, with the maximum at lower viscosity and stenosis height and the minimum at higher viscosity and stenosis height, signifies the complex interaction between blood viscosity, stenosis induced narrowing, and resistance to flow. The physical significance of this observation is the amplification of viscous dissipation, which results in slower blood flow and reduced efficiency in nutrient and oxygen transport, particularly in constricted arteries.

The volumetric flow rate is primarily influenced by stenosis height and blood viscosity. Stenosis height plays a dominant role in restricting flow as the artery narrows, while viscosity impacts flow more significantly in minimally stenosed arteries. As stenosis height increases, artery narrowing becomes the key factor limiting flow. Hematocrit and curvature have secondary effects, especially in severely stenosed conditions. Therefore, artery geometry (stenosis and curvature) and blood viscosity (due to hematocrit and red blood cells) govern the flow dynamics, with stenosis height being the most influential factor in constricted

3.3 Pressure drop across a curved stenotic artery

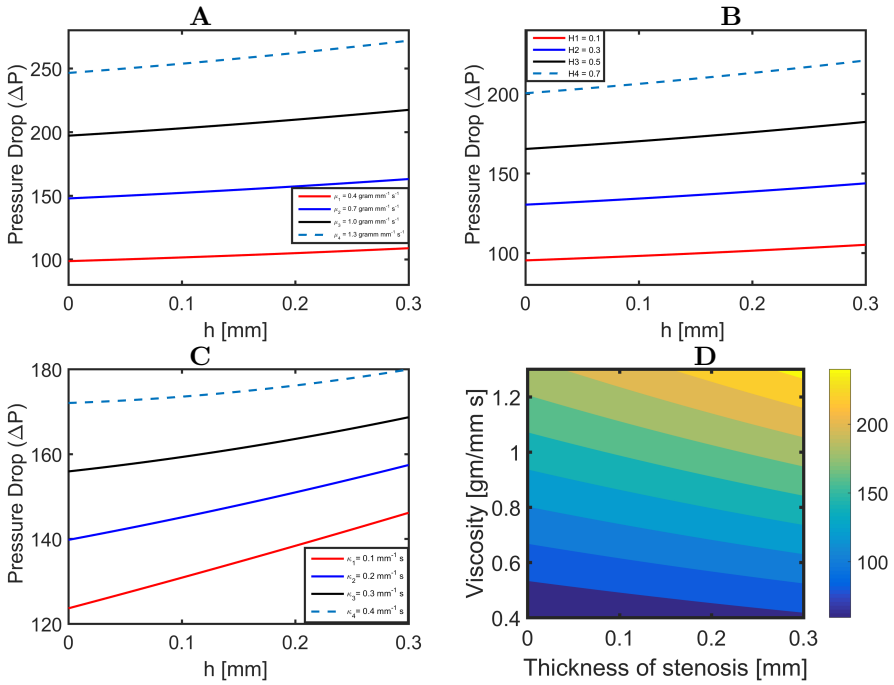

Figure 4: Pressure drop variations with thickness of stenosis for **A:** different viscosities, **B:** various hematocrit, **C:** various curvature.

Figure 4A the change of pressure drop and h for different values of viscosity shows almost linear lines because the interval taken here is very small, though they are actually parabolic curves. The pressure drop values is measured when h lies between 0 and 0.3 mm. The figure shows that the pressure drop is maximum, about 271.4 mm of Hg, when the viscosity is 1.3 gram mm^{-1} s^{-1} at $h = 0.3$ mm. The pressure drop are approximately $(98.56, 147.8, 197.1, 246.4)$ mm of Hg for the viscosity values $(0.4, 0.7, 1.0, 1.3)$ gram mm^{-1} s^{-1} respectively at $h = 0$. Similarly, the drops are $(108.9, 163.9, 217.5, 271.4)$ for viscosity values of $(0.4, 0.7, 1.0, 1.3)$ gram mm^{-1} s^{-1} respectively at $h = 0.3$ mm. The pressure drop increases approximately

linearly within the given small interval, reflecting the combined effect of increased resistance to flow due to higher viscosity and the narrowing of the arterial vessel. From a biomechanics perspective, the increasing pressure drop indicates enhanced frictional resistance as blood flow encounters greater viscosity and a constricted artery, which impedes the normal hemodynamics and could lead to higher cardiovascular risks in clinical conditions.

Figure 4B the change in the pressure drop and h for different values of hematocrit shows almost linear lines because the interval taken here is very small, though they are actually parabolic curves. The pressure drop values is measured when h lies between 0.0 and 0.3 mm. The figure shows that the pressure drop is maximum, about 221 mm of Hg, when the hematocrit is 0.7 at $h = 0.3$ mm. The pressure drop are approximately $(95.32, 130.3, 165.3, 200.4)$ mm of Hg for hematocrit values of $(0.1, 0.3, 0.5, 0.7)$ respectively at $h = 0$. Similarly, the drops are $(105.1, 143.7, 182.3, 221)$ mm of Hg for hematocrit values of $(0.1, 0.3, 0.5, 0.7)$ respectively at $h = 0.3$ mm. This data highlights how higher hematocrit levels cause a higher volume fraction of red blood cells, which increases the blood's viscosity and resistance to flow, contributing to greater pressure drops in the artery. This information is significant for understanding the role of hematocrit in cardiovascular conditions.

Figure 4C the change in the pressure drop and h for different values of curvature shows some how linear because the interval taken here is very small, though they are actually parabolic curves. The pressure drop values is measured when h lies between 0 and 0.3 mm. The figure shows that the pressure drop is maximum, about 179.9, when the curvature is 0.4 mm^{-1} s at $h = 0.3$ mm. The pressure drop is approximately 123.8 mm of Hg for the curvature value 0.1 mm^{-1} s at $h = 0$. Similarly, it is 139.8 mm of Hg for 0.2 mm^{-1} s and nearly 155.9 mm of Hg for 0.3 mm^{-1} s at $h = 0$ respectively. This result highlights the significance of arterial geometry in determining flow resistance, where greater curvature causes higher resistance due to the additional centrifugal forces acting on the fluid. Increased curvature also amplifies the effect of stenosis, restricting the flow further and leading to higher pressure drops. The physical implication is that, as curvature increases, the flow faces greater resistance, particularly in narrowed arteries, affecting blood circulation and potentially contributing to adverse cardiovascular effects.

Figure 4D, describes the distribution of pressure drop for different values of viscosity and thickness of stenosis. Viscosity μ takes vlues $(0.4, 0.7, 1.0, 1.3$ gram mm^{-1} s^{-1}. Thickness of stenosis has values $(0, 0.1, 0.2, 0.3)$ mm. The pressure drop ΔP at $h = 0$ and $\mu_1 = 0.4$ gram mm^{-1} s^{-1} is 59.52 mm of Hg . As the thickness increases the pressure drop is also increases for the same viscosity and becomes 77.05 mm of Hg at $h = 0.3$ mm. The pressure drop at $h = 0.3$ mm is 189.2 mm of Hg for the viscosity 1 gram mm^{-1} s^{-1} and becomes 245.5 at $\mu_4 = 1.3$gram mm^{-1} s^{-1} for the same thickness. The pressure drop at $h = 0.1$ mm are $(64.56, 113.5, 161.3, 209.3)$ mm of Hg for the viscosity $(0.4, 0.7, 1.0, 1.3)$ gram mm^{-1} s^{-1} respectively. The pressure drop are $77.05, 134.6, 189.2, 245.5$ mm of Hg at $h = 0.3$ mm for the viscosities $(0.4, 0.7, 1.0, 1.3)$ gram mm^{-1} s^{-1} respectively. This combined effect leads to an increase in pressure drop, indicating that both viscosity and stenosis thickness significantly contribute to the impedance of blood flow. The physical interpretation is that higher viscosity due to increased red blood cell concentration or plasma viscosity, alongside increased stenosis thickness, worsens flow resistance, which could lead to higher pressure on the arterial walls and contribute to conditions like hypertension.

The pressure drop in stenosed arteries increases with higher viscosity, hematocrit, curvature, and stenosis thickness. Viscosity and hematocrit amplify flow resistance by enhancing blood's internal friction, while stenosis thickness directly restricts the arterial passage. Increased curvature worsen pressure drops due to centrifugal forces, intensifying resistance in curved arteries. Curvature provides more realistic results as it captures the combined effects of geometric constraints and flow dynamics, reflecting actual physiological conditions more accurately.

3.4 Shear stress across a curved stenotic artery

Figure 5A the change of shear stress and h for different values of viscosity shows almost linear lines because the interval taken here is very small, though they are actually parabolic curves. The shear stress values is measured when h lies between 0 and 0.3 mm. The figure shows that the shear stress is maximum, about 188.4 gram mm^{-1} s^{-2}, when the viscosity is 1.3 gram mm^{-1} s^{-1} at $h = 0.3$ mm. The shear stress are approximately $(69.37, 104, 138.7, 173.4)$ gram mm^{-1} s^{-2} for the viscosity values $(0.4, 0.7, 1.0, 1.3)$ gram

mm^{-1} s^{-1} respectively at $h = 0$. Similarly, the stress are $(75.35, 113, 150.7, 188.4)$ gram mm^{-1} s^{-2} for viscosity values of $(0.4, 0.7, 1.0, 1.3)$ gram mm^{-1} s^{-1} respectively at $h = 0.3$ mm. The increase in shear stress reflects greater frictional forces at the arterial walls due to elevated viscosity and narrowing of the lumen from stenosis. This heightened shear stress could contribute to endothelial damage and vascular remodeling, emphasizing its role in the progression of cardiovascular diseases.

Figure 5B the change in the shear stress and h for different values of hematocrit is analyzed. The lines appear almost approximately linear because the interval taken here is very small, though they are actually parabolic curves. The shear stress values is measured when h lies between 0 and 0.3 mm. The figure shows that the shear stress is maximum, about 155.4 gram mm^{-1} s^{-2}, when the hematocrit is 0.7 at $h = 0.3$ mm. The shear stress are approximately $(69.32, 97.62, 120.3, 145.7)$ gram mm^{-1} s^{-2} for hematocrit values of $(0.1, 0.3, 0.5, 0.7)$ respectively at $h = 0$. Similarly, they are $(73.91, 104.1, 128.2, 155.4)$ gram mm^{-1} s^{-2} for hematocrit values of $(0.1, 0.3, 0.5, 0.7)$ respectively at $h = 0.3$ mm. The elevated hematocrit increases the red blood cell concentration, leading to higher blood viscosity, which in turn raises the shear stress at the arterial wall. This elevated shear stress can induce endothelial strain and disrupt normal vascular function, potentially contributing to the development of cardiovascular disorders.

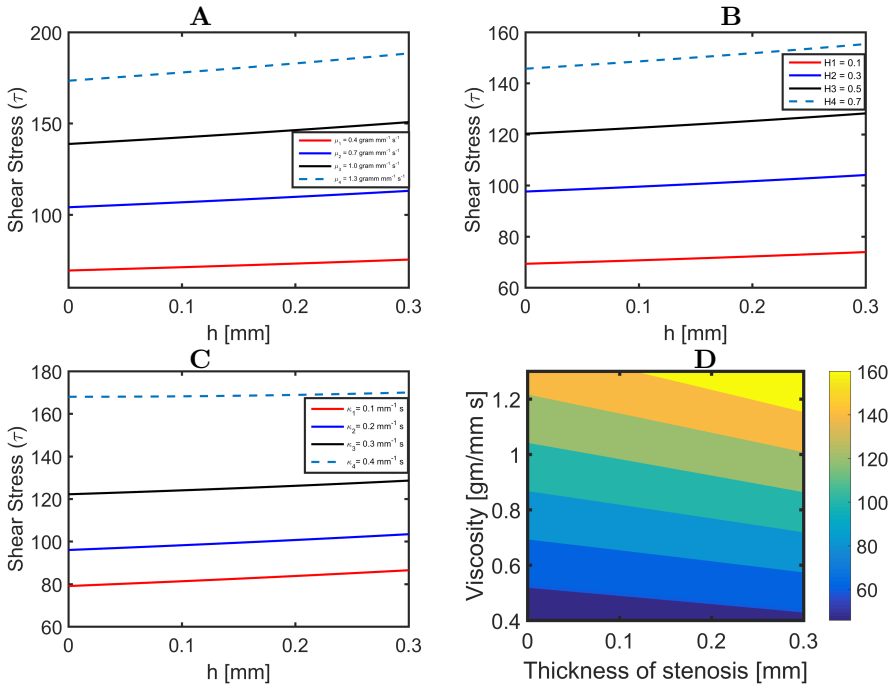

Figure 5: Shear stress variations with thickness of stenosis for **A:** different viscosities, **B:** various hematocrit, **C:** various curvature.

Figure 5C the change in the shear stress and h for different values of curvature is analyzed. The lines appear almost linear because the interval taken here is very small. The shear stress values is measured when h lies between 0 and 0.3 mm. The figure shows that the shear stress is maximum, about 170 gram mm^{-1} s^{-2}, when the curvature is 0.4 mm^{-1} s. The shear stress is approximately 79.06 gram mm^{-1} s^{-2} for the curvature value 0.1 mm^{-1} s at $h = 0$. Similarly, it is 96 gram mm^{-1} s^{-2} for 0.2 mm^{-1} s and nearly 122.2 for 0.3 mm^{-1} s. The increased curvature introduces enhanced centrifugal forces, causing greater resistance to blood flow and elevating shear stress at the arterial walls. This phenomenon, particularly in stenosed regions, may disrupt normal hemodynamic patterns, induce vascular remodeling, and contribute to localized endothelial damage, emphasizing the importance of arterial geometry in cardiovascular risk assessments.

Figure 5D, describes the distribution of shear stress for different values of viscosity and thickness of stenosis.

Viscosity μ takes vlues $(0.4, 0.7, 1.0, 1.3$ gram mm^{-1} s^{-1}. Thickness of stenosis has values $(0, 0.1, 0.2, 0.3)$ mm. The shear stress τ at $h = 0$ and $\mu_1 = 0.4$ gram mm^{-1} s^{-1} is 45.84 gram mm^{-1} s^{-2}. As the thickness increases the shear stress is also increases for the same viscosity and becomes 55.25 gram mm^{-1} s^{-2} at $h = 0.3$ mm. The shear stress at $h = 0.3$ mm is 138.4 gram mm^{-1} s^{-2} for the viscosity 1 gram mm^{-1} s^{-1} and becomes 179.5 gram mm^{-1} s^{-2} at $mu_4 = 1.3$ gram mm^{-1} s^{-1} for the same thickness. The shear stress at $h = 0.1$ mm are $(48.67, 85.42, 122.1, 157.8)$ gram mm^{-1} s^{-2} for the viscosity $(0.4, 0.7, 1.0, 1.3)$ gram mm^{-1} s^{-1} respectively. The shear stress are $55.25, 96.82, 138.4, 179.5$ gram mm^{-1} s^{-2} at $h = 0.3$ mm for the viscosities $(0.4, 0.7, 1.0, 1.3)$ gram mm^{-1} s^{-1} respectively. This trend reflects the combined effects of increased viscosity, which heightens internal resistance, and stenosis thickness, which narrows the arterial passage, amplifying wall shear stress. Biomechanically, elevated shear stress can lead to endothelial dysfunction, promote plaque formation, and increase the risk of arterial damage.

The analysis of shear stress variations due to viscosity, hematocrit, curvature, and stenosis thickness highlights key biomechanical insights. Elevated viscosity and hematocrit increase shear stress by amplifying blood's internal resistance, whereas curvature induces centrifugal forces, disrupting flow and intensifying stress on arterial walls. Stenosis further worsen these effects by narrowing the lumen, enhancing frictional forces. These findings emphasize the interplay between blood rheology and arterial geometry in influencing vascular stress. Including axial curvature in the model provides a more realistic representation of arterial hemodynamics, aiding in better understanding cardiovascular risk factors and endothelial responses.

4 Conclusion

This work investigates the hemodynamic effects of atherosclerotic plaque-induced stenosis on blood flow dynamics, focusing on the role of radial blood viscosity and artery curvature. By incorporating effective viscosity into the Navier-Stokes equations in cylindrical polar coordinates with sinusoidal geometry, analytical expressions for the velocity profile, volumetric flow rate, pressure drop, and shear stress in curved arteries are derived. The results show that increasing curvature, hematocrit, viscosity, and the position of stenosis reduces the hemodynamic parameters. A uniform increase in hematocrit, viscosity, and curvature leads to a decline in velocity and volumetric flow rate and proportional increases in pressure drop and shear stress, with curvature and hematocrit primarily influencing shear stress and viscosity dominating pressure drop. These findings highlight the importance of effective viscosity in determining blood flow parameters and the risk of occlusion due to stenosis.

References

[1] Alizadehard, D., Imai, Y., Nakaaki, K., Ishikawa, J., and Yamaguchi, T., 2012, Quantification of red blood cell deformation at high hematocrit blood flow in microvessels, *Journal of Biomechanics,* 44(15), 2684-2689.

[2] Bali, R., and Awasthi, U., 2007, Effects of magnetic field on the resistance to blood flow through stenosed artery, *Appl. Math. Comput.,* 188, 1635-1641.

[3] Biswas, D., and Chakravarty, U. S., 2010, Impact of hematocrit and slip velocity on pulsatile blood flow in a constricted tapered artery, *International Journal of Engineering Research and Technology,* 3(3), 435-449.

[4] Biwas, D., and Paul, N., 2013, Study of blood flow inside an inclined non-uniform stenosed artery, *Int. J. of Mathematicle Archive,* 4, 33-42.

[5] Chakravarty, S., and Chaudhary, A. G., 1988, Response of blood flow through an artery under stenotic conditions, *Rheologica Acta,* 27, 418-427.

[6] Chakravarty, S., 1987, Effects of stenosis on the flow-behaviour of blood in an artery, *International journal of Engineering Science,* 25, 1003-1016.

[7] Chaturani, P. R., and Ponalagusamy, R., 1985, A study of non-Newtonian aspects of blood flow through stenosed arterties and its applications in arterial diseases, *Biorheology,* 22, 521-531.

[8] Dash, R. K., Jayaraman, G., and Mehta, K. N., 1999, Flow in a catherized curved artery with stenosis, *Journal of Bio-mechanics,* 32, 49-61.

[9] Diwakar, C., and Kumar, S., 2016, Effects of axially symmetric stenosis on the blood flow in an artery having mild stenosis, *IJMTT,* 35, 163-167.

[10] Ellah, R., and Rahman, S. U., 2013, The theoretically study of unsteady blood flow of jeffery fluid through a stenosed arteries with permeable walls, *Zeatschr Naturforchung,* 489-498.

[11] Forrester, J. H., and Young, D. F., 1970, Flow through a converging-diverging tube and its implications in occlusive vascular diseaseai theoretical development, *J. Biomech.,* 3, 297-305.

[12] Gautam, P. N., Pokharel, C., Phaijoo, G. R., Kattel, P., and Kafle, J., 2023, Effect of increasing stenosis over time on hemodynamics, *Journal of Biomath,* 2(12), 1-10.

[13] Haldar, K., and Andersson, H. I., 1996, Two layered model of blood flow through stenosed arteries, *Acta Mechanica,* 117, 221-228.

[14] Harjeet, K., Chandel, R. S., and Sanjeet, K., 2013, A mathematical model for blood flow through a narrow catheterized artery, *International Journal Theoretical and Appl. Sci.,* 5(2), 101-108.

[15] Jain, M., Sharma, G. C., and Singh, R., 2010, Mathematical modeling of blood flow in a stenosed artery under MHD effect through porous medium, *International Journal of Engineering,* 23, 243-251.

[16] Kafle, J., Gaire, H. P., Pokherel, P. R., and Kattel, P., 2022, Analysis of blood flow through curved artery with mild stenosis, *Mathematical Modeling and Computing,* 9, 217-225.

[17] Kapur, J. N., 1985, Mathematical models in biology and medicine, In: Models for blood flows, *Affiliated East-West Press Pvt. Ltd. India,* 347.

[18] Liepsch, D., 2002, An introduction to mechanics, basic models and applications, *Journal of Bio-mechanics,* 35, 415-435.

[19] Lih, M. M., 1996, Transport phenomenon in medicine and biology, *John Wiley and Sons, New York: NY, USA,* 184(1), 198-200.

[20] MaCdonald, D., 1979, On steady flow through modelled vascular stenosis, *J. Biomech.,* 12, 13-20.

[21] Mandal, P. K., and Chakravarty, S., 2007, Numerical study of unsteady flow of non-Newtonian fluid through different shaped arterial stenosis, *International Journal of Computer Mathematics,* 84, 1059-1077.

[22] Misra, J. C., Patra, M. K., and Sahu, B. K., 1992, Unsteady flow of blood through narrow blood vessels: A mathematical analysis, *Computer Math. Appli.,* 24(10), 19-31.

[23] Nosovitsky, V. A., Ilegbusi, O. J., Jiang, J., Stone, P. H., and Feldman, C. L., 1997, Effects of curvature and stenosis-like narrowing on wall shear stress in a coronary artery model with phasic flow, *Computers and Biomedical Research,* 30, 61-82.

[24] Onitilo, S. A., and Usman, M. A., 2018, Mathematical analysis of blood flow through a stenosed human artery, *Annals. Computer Science Series,* 16(2), 177-185.

[25] Onitilo, S. A., and Usman, M. A., 2021, *Effect of multiple stenosis on blood flow in human artery, Fuw Trends in Science and Tech.,* 6(2), 643-649.

[26] Pokharel, C., Gautam, P. N., Tripathee, S. T., Bhatta, C. R., and Kafle, J., 2022, Analysis of flow parameters in blood flow through mild stenosis, *Nepalese Journal of Zoology*, 6(2), 39-44.

[27] Pokharel, C., Kafle, J., and Bhatta, C. R., 2024, Analysis of flow characteristics of the blood flow through curved artery with mild stenosis, *Journal of Jilin University (Engineering and Technology Edition),* 43(3), 155-169.

[28] Pokharel, C., Gautam, P. N., Bhatta, C. R., and Kafle, J., 2024, Analysis of blood flow through stenosed artery with Einstein viscosity, *Journal of Tianjin University Science and Technology,* 57(4), 36-52.

[29] Pokharel, C., Pokharel, S., Upadhyay, A., and Upadhyay, B., 2024, Analysis of blood flow through stenosed curved artery with Einstein viscosity, *Communications on Applied Nonlinear Analysis,* 31(3s), 169-185.

[30] Pokharel, C., Gautam, P. N., Bhatta, C. R., and Kafle, J., 2024, Analysis of hemodynamic parameters on two-layered blood flow in a curved artery, *Biomath,* 13, 2406286, 1-15.

[31] Padmanabhan, N., and Jayaraman, G., 1984, Flow in a curved tube with constriction - an application to the arterial system, *Medical and Biological Engineering and Computing,* 22(3), 216-224.

[32] Qiu, Y., and Trabell, J. M., 2000, Numerical simulations of oxygen mass transfer in a compliant curved tube model of a coronary artery, *Annals of Biomedical Engineering,* 28, 26-38.

[33] Samundra, T. T., and Kafle, J., 2023, Analysis of effect of hemodynamic parameters on two-layerd blood flow in a mild stenosed artery, *The Nepali Math Science Report, Central Department of Mathematics, TU, Nepal,* 35(1 and 2), 25-37.

[34] Singh, A. K., 2012, Effects of Shape Parameter and Length of Stenosis on Blood Flow through Improved Generalized Artery with Multiple Stenoses, *Advances in Applied Mathematical Bio-sciences,* 3, 41-48.

[35] Seeley, B. D., and Young, D. F., 1976, Effect of geometry on pressure losses across models of arterial stenosis, *Journal of Bio-mechanics,* 9, 447-448.

[36] Schilt, S., Moore, J. E., Delfino, A., and Meister, J. J., 1996, The effects of time-varying curvature on velocity profiles in a model of the coronary arteries, *Journal of Bio-mechanics,* 29, 469-474.

[37] Santamarina, A., Weydahl, E., Siegel, J. M., and Moore, J. E., 1998, Computational analysis of flow in a curved tube model of the coronary arteries: Effects of time-varying curvature, *Annals of Biomedical Engineering,* 26(1), 944-954.

[38] Srivastava, V. P., and Rastogi, R., 2010, Blood flow through a stenosed catheterized artery: Effects of hematocrit and stenosis shape, *Computers and Mathematics with Applications,* 59(4), 1377-1385.

[39] Srivastava, V. P., and Rastogi, R., 2009, Effects of hematocrit on impedance and shear stress during stenosed artery catheterization, *Applications and Applied Mathematics,* 4(1), 98-113.

[40] Srivastava, V. P., 2002, Particulate suspension blood flow through stenotic arteries, effects of hematocrit and stenosis shape, *Indian J. Pure appl. Math.,* 33, 1353-1360.

[41] Verma, N., and Parihar, R. S., 2009, Effects of magneto-hydrodynamic and hematocrit on blood flow in an artery with multiple mild stenosis, *Int. J. Appl. Math. Comput.,* 1, 30-46

[42] Young, D. F., and Tsai, F. Y., 1973, Flow characteristic in models of arterial stenosis-II, Unsteady flow, *Journal of Bio-mechanics,* 6, 547-559.